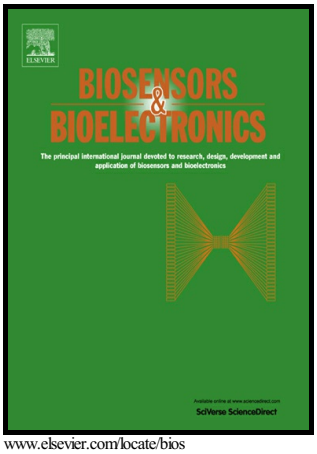

www.elsevier.com/locate/bios

Antibody functionalized graphene biosensor for label-free electrochemical immunosensing of fibrinogen, an indicator of trauma induced coagulopathy

Waqas Saleem, Carlos Salinas, Brian Watkins, Gavin Garvey, Anjal C. Sharma, Ritwik Ghosh

PII: S0956-5663(16)30637-6
DOI: http://dx.doi.org/10.1016/j.bios.2016.07.009
Reference: BIOS8890

To appear in: *Biosensors and Bioelectronic*

Received date: 9 May 2016
Revised date: 25 June 2016
Accepted date: 4 July 2016

Cite this article as: Waqas Saleem, Carlos Salinas, Brian Watkins, Gavin Garvey, Anjal C. Sharma and Ritwik Ghosh, Antibody functionalized graphene biosenso for label-free electrochemical immunosensing of fibrinogen, an indicator o trauma induced coagulopathy, *Biosensors and Bioelectronic* http://dx.doi.org/10.1016/j.bios.2016.07.009

Antibody functionalized graphene biosensor for label-free electrochemical immunosensing of fibrinogen, an indicator of trauma induced coagulopathy.

Waqas Saleem, Carlos Salinas, Brian Watkins, Gavin Garvey, Anjal C. Sharma* and Ritwik Ghosh*

Lynntech, Inc., 2501 Earl Rudder Fwy S., College Station, TX 77845, USA.

*Corresponding authors.

E-mail address: ritwik.ghosh@lynntech.com Tel. +1 979 764 2316; fax: +1 979 764 2343

E-mail address: anjal.sharma@lynntech.com Tel. +1 979 764 2317; fax: +1 979 764 2343

Abstract

An antibody, specific to fibrinogen, has been covalently attached to graphene and deposited onto screen printed electrodes using a chitosan hydrogel binder to prepare an inexpensive electrochemical fibrinogen biosensor. Fourier Transform Infrared (FT-IR) spectroscopy has been utilized to confirm the presence of the antibody on the graphene scaffold. Electrochemical Impedance Spectroscopy (EIS) has been utilized to demonstrate that the

biosensor responds in a selective manner to fibrinogen in aqueous media even in the presence of plasminogen, a potentially interfering molecule in the coagulopathy cascade. Furthermore, the biosensor was shown to reliably sense fibrinogen in the presence of high background serum albumin levels. Finally, we demonstrated detection of clinically relevant fibrinogen concentrations (938 – 44542 μg/dL) from human serum and human whole blood samples using this biosensor. This biosensor can potentially be used in a point-of-care device to detect the onset of coagulopathy and monitor response following therapeutic intervention in trauma patients. Thus this biosensor may improve the clinical management of patients with trauma-induced coagulopathy.

Key words: Graphene; Fibrinogen; Antibody attached graphene biosensor; Trauma-induced coagulopathy; Continuous fibrinogen monitoring

1. Introduction

Traumatic injury represents one of the most common reasons for mortality and accounts for 14.2% of all fatalities (D'Angelo *et al*. 2010). Approximately one-quarter of all trauma related hospital admissions present with coagulopathy (Brohi *et al*. 2008). About 40% of trauma-related deaths are related to rapid onset of coagulopathy and hemorrhagic shock, and the vast majority of trauma patients are coagulopathic at the time of death (Sauaia *et al*. 1995). This problem is not confined to civilians only, as a study of US military death distribution indicates that 91.5% of potentially survivable deaths in warzones were due to battlefield trauma-induced coagulopathy (Pusateri 2012). Trauma-induced coagulopathy is characterized by severe blood loss along with enhanced consumption of clotting factors and platelets. Additionally,

hyperfibrinolysis, hypothermia, acidosis and metabolic changes can also hinder the coagulation system (D'Angelo *et al*. 2010). These events directly affect fibrinogen polymerization (Fries *et al*. 2010). In trauma-induced hemorrhage, fibrinogen is a crucial component that reaches a critical value earlier than other procoagulatory factors and platelets (Fries *et al*. 2010, Nardi *et al*. 2013). Decrease of fibrinogen below a threshold value is associated with poor outcomes (Nardi *et al*. 2013). Additionally, survival following traumatic injury-induced severe blood loss improves following fibrinogen administration (Stinger 2008). Therefore, a point-of-care diagnostic that enables continuous monitoring of fibrinogen could empower the attending physician with clinically actionable information. Such information could potentially guide fibrinogen replacement therapy and thereby prevent the onset of, or reverse, trauma-induced coagulopathy. This in turn could potentially greatly improve the chances of survival of trauma patients, both in the civilian as well as in the military medical care setup.

Clinical laboratory assays such as the Clauss assay, prothrombin-derived fibrinogen assay, immunological assays, gravimetric assays and thromboelastrograms can accurately quantify fibrinogen from patient provided blood or plasma samples (Meyer *et al.* 2015, Undas 2016). However, these assays are quite complicated, time consuming, involve multiple steps and require sophisticated laboratory instrumentation and trained personnel to perform. Moreover, fibrinogen quantification is not achieved in near real-time using these assays. Therefore, these assays cannot be directly translated to point-of-care fibrinogen monitoring devices. An ideal point-of-care fibrinogen monitoring device should be compact, lightweight and automated. Furthermore, it should incorporate a fibrinogen sensing approach that is inexpensive, reliable and capable of functioning in unprocessed whole blood samples. Finally, the sensing approach utilized must be able to provide a near real-time quantification to enable temporal resolution of

fibrinogen concentration at physiologic timescales in order to guide fibrinogen replacement therapy.

Herein, we describe for the first time, a label-free fibrinogen sensing approach that could potentially fulfill the above criteria for point-of-care continuous fibrinogen monitoring from unprocessed whole blood samples. We have utilized graphene as the scaffold, upon which to build our fibrinogen biosensor. Graphene, an allotropic form of carbon and a two-dimensional honeycomb lattice of sp^2 hybridized carbon atoms, exhibits very high electron mobility (200,000 cm^2/Vs), high saturation velocity (~4.5E7 cm/s), high carrier concentration (10E13/cm^2), large current densities (~3E9 A/cm^2) due to confinement of electrons in two dimensions, and exceptional mechanical strength (Liu *et al*. 2012). These features of graphene make it ideal as a scaffold for novel electrochemical biosensors. Fibrinogen selective antibodies covalently attached to a graphene scaffold were prepared and were deposited onto inexpensive screen printed electrodes to construct fibrinogen biosensors. FT-IR spectroscopy was utilized to confirm the presence of the antibodies on the graphene scaffold and hence the biosensor. Electrochemical impedance spectroscopy was utilized to demonstrate that these electrodes are selective label-free immunosensors for fibrinogen and can be used to detect fibrinogen from aqueous media. The biosensor selectively senses fibrinogen in the presence of a potentially interfering coagulation cascade molecule, plasminogen, and in the presence of high background serum albumin levels. We have utilized this biosensor to sense fibrinogen spiked in human serum and unprocessed blood samples, over the clinically relevant range (938 – 44542 μg/dL) of fibrinogen concentrations encountered in coagulopathic patients (Fries *et al*. 2010, Nardi *et al*. 2013). The limit of detection with this biosensor is estimated at ~ 500 μg/dL of fibrinogen in serum and blood but could be further decreased upon biosensor optimization. This biosensor

could therefore potentially improve the clinical management of trauma patients by providing a means for near real-time detection of the onset of coagulopathy and monitoring patient response following therapeutic interventions.

2. Materials and Methods

2.1. Materials and reagents

Fibrinogen specific antibody 12HC was procured from Thermo-Fisher Scientific (Waltham, MA, USA). Plasminogen-depleted fibrinogen from human plasma, human plasminogen from fresh human plasma, human fibrinogen ELISA kit, and single donor human whole blood were purchased from Innovative Research (Novi, MI, USA). Defibrinated human serum was obtained from Golden West Biologicals, Inc. (Temecula, CA, USA). Aminated graphene amino-PEG covalently linked was sourced from ACS Materials Corporation (Medford, MA, USA). Succinic acid, N-hydroxyl succinimide (NHS), N-(3-Dimethylaminopropyl)-N′-ethylcarbodiimide hydrochloride (EDC), FT-IR grade Potassium Bromide (KBr), chitosan, Bovine Serum Albumin (BSA), Human Serum Albumin (HSA), potassium ferrocyanide and potassium ferricyanide were procured from Sigma-Aldrich Corporation (St. Louis, MO, USA). ET083-40 Zensor SE100 SPE screen printed electrodes were sourced from eDAQ Corporation (Colorado Springs, CO, USA). Ag/AgCl reference electrodes and Pt wire counter electrodes were purchased from CH Instruments, Inc. (Austin, TX, USA).

2. 2. Preparation and characterization of 12HC antibody attached graphene (12HC-G)

A simple three step functionalization process, modified from a reported method (Sharma *et al.* 2004) and schematically depicted in Fig. 1, was utilized to covalently attach the 12HC

antibody specific for fibrinogen onto the graphene scaffold. Our rationale for the selection of fibrinogen specific antibody 12HC is presented in the supplementary information, Table S1 and Fig. S1. First, 100 mg of aminated graphene (amino-PEG covalently linked) was suspended in 9 mL of deionized water. Succinic acid (0.024 g, 0.2032 mmol) and EDC (0.038g, 0.1982 mmol) was added to the suspension and stirred for 60 min. The suspension was centrifuged to cause the graphene material to settle but not form a tightly packed pellet and supernatant discarded. The carboxyl modified graphene was thoroughly washed by five cycles of resuspension in 10 mL of deionized water, vortex agitation for 5 min, centrifugation and supernatant removal. Then, the carboxyl modified graphene was resuspended in 10 mL of 0.1M MES buffer at pH 6.0. NHS (0.023 g, 0.1998 mmol) and EDC (0.038 g, 0.1982 mmol) were added to the suspension and stirred for 45 minutes. The suspension was washed thrice as above *via* centrifugation, supernatant removal and resuspension in PBS (10 mM phosphate, 138 mM NaCl, pH 7.4) to remove excess NHS and reaction byproducts to obtain the intermediate NHS adduct. Finally, 15 μL of 12HC antibody solution (0.5 mg/mL in PBS) was added to the PBS suspension of the intermediate NHS adduct and placed in a refrigerator at 4 °C overnight. The suspension was washed thrice as above *via* centrifugation, supernatant removal and resuspension in PBS to remove excess antibody and released NHS. Final resuspension was in 5 mL of PBS resulting in a 12HC antibody attached graphene (12HC-G) suspension weight per volume of 18 mg/mL.

KBr pellets of the starting aminated graphene and the 12HC-G materials were prepared by mixing 2 mg of graphene material in 98 mg of KBr and finely grinding in an agate mortar with an agate pestle. The freely flowing homogenous mixture was added between two dies in a die holder and subjected to mechanical pressure of 6 KPa in a Carver hydraulic press, at room temperature for 10 minutes in order to obtain thin and translucent KBr pellets. These pellets

were utilized to obtain FT-IR spectra using a Bruker Tensor 27 FT-IR instrument. The FT-IR spectrum of each graphene material was collected at a spectral resolution of 4 cm^{-1} with 2048 transients collected to obtain good signal-to-noise ratio over the entire spectral range of 400 cm^{-1} – 4000 cm^{-1}. The background subtracted spectra were saved as comma delimited ASCII-text files with 1866 discrete data points per file and exported into Microsoft Excel 2007 for spectral plot preparation and peak assignment operations.

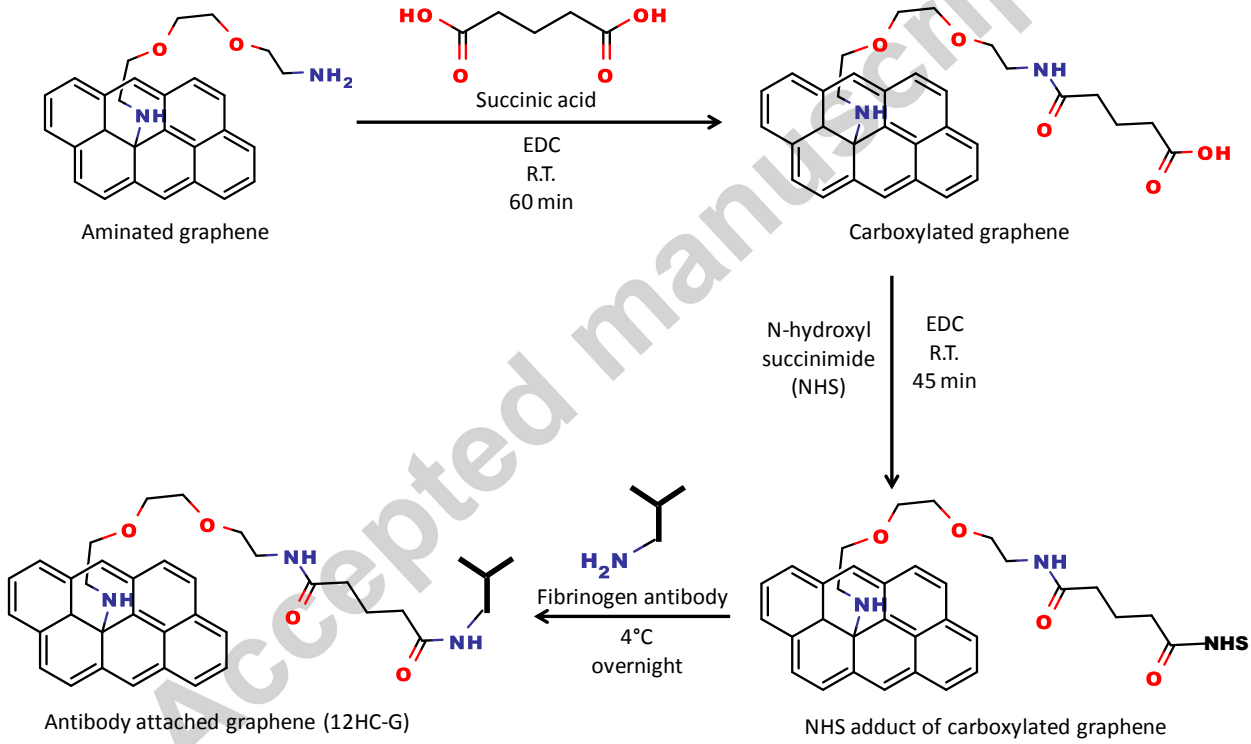

Fig. 1. Simple three step coupling chemistry to prepare fibrinogen selective antibody 12HC attached graphene.

2. 3. Deposition of 12HC-G on screen printed electrodes to obtain fibrinogen biosensor

Inexpensive and disposable screen printed graphitic electrodes (Zensor SE100) were utilized to prepare the fibrinogen biosensor. These electrodes were first treated with either low pressure air plasma in a plasma cleaner (Harrick Scientific model PDC-32G) operated at 40

mTorr pressure at 6.8 W RF power for 2 minutes, or with our in-house 3% air-in-helium, non-thermal atmospheric pressure plasma jet set-up (Parkey *et al*. 2015) at applied voltage of 5.8 kV for 2 minutes. Gas plasma treatment modifies the graphitic electrode, creating a more hydrophilic surface and enabling thorough wetting with aqueous media. The 12HC-G suspension (18 mg/mL) was briefly agitated to ensure homogenous distribution of the graphene material. A small aliquot of the suspension (15 μL) was deposited on the electrode surface, followed by addition of 2 μL of 1% chitosan solution to the suspension and gentle mixing to ensure homogeneous distribution of the chitosan hydrogel binder throughout the suspension. The electrode with the 12HC-G deposited on its surface was allowed to air dry overnight and washed thoroughly with PBS to remove excess chitosan. The surface of the 12HC-G deposited electrode was then blocked with 5% BSA solution in PBS for 1 hour to ensure that non-specific binding of other species is minimized and signal response mainly derives from fibrinogen challenge. This was followed by thorough washing with PBS to remove excess BSA, to obtain the 12HC-G biosensors, which were stored in PBS at 4 °C in a refrigerator. Graphene only electrodes (no covalently attached 12HC antibodies) were prepared in a similar fashion as controls. Fig. 2 schematically depicts the fibrinogen biosensor preparation process and the principle behind impedimetric sensing of fibrinogen with this biosensor. The effect of gas plasma treatment on the screen printed electrode surfaces is presented in the supplementary information, Fig. S3. The necessity for chitosan hydrogel binder to keep the graphene material firmly deposited onto the electrode surface is also presented in the supplementary information, Fig. S4.

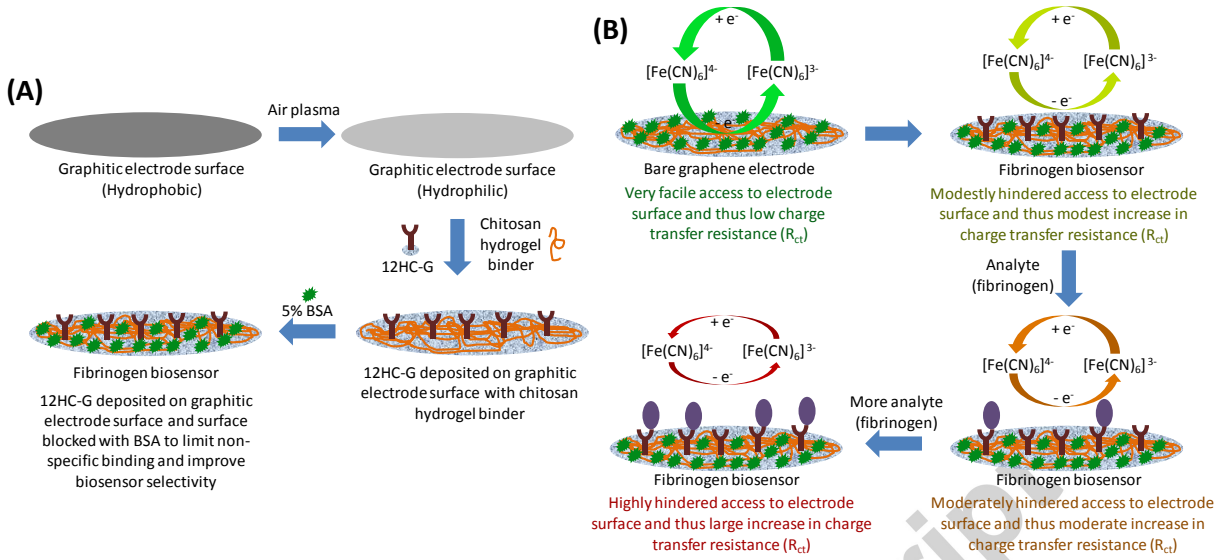

Fig. 2. (A) Preparation of fibrinogen biosensor by deposition of 12HC-G followed by blocking with BSA. (B) Principle of fibrinogen sensing with the biosensor. As more fibrinogen is bound to the antibodies, surface access is hindered which is manifested as increasing charge transfer resistance as seen *via* EIS spectroscopy.

2. 4. Electrochemical impedance spectroscopy (EIS) for sensing fibrinogen with biosensor

A miniature three-electrode electrochemical cell (supplementary information, Fig. S5) was utilized to determine the response of the biosensor to fibrinogen using EIS spectroscopy as the read-out method. The electrolyte utilized was PBS containing 5 mM each of potassium ferrocyanide and potassium ferricyanide as the redox indicator. In this set-up, the biosensor acts as the working electrode, a standard Ag/AgCl electrode acts as the reference electrode and a Pt wire acts as the counter electrode. A VersaStat MC 4-channel potentiostat/galvanostat and associated VersaStudio v2.40.4 control software suite was used to interrogate the electrodes *via* EIS in the miniature electrochemical cell. For all experiments, the sweep frequency range was from 0.01 – 100,000 Hz and the software enabled measurement of -Z" / Ohm and Z' / Ohm, over this sweep frequency range. Fibrinogen as obtained is in an aqueous solution format at a concentration of 44.44 mg/mL.

Incrementally increasing aliquots (2, 4 and 10 μL) of this fibrinogen solution were added into 10 mL of the electrolyte solution containing the biosensor and the response from the biosensor after each incremental fibrinogen addition was recorded.

Plasminogen as obtained was in 0.1M HEPES and 0.1M NaCl pH 7.4 aqueous solution at a concentration of 10 mg/mL. In separate experiments, incrementally increasing aliquots (8, 16 and 24 μL) of plasminogen were first added to 6 mL of the electrolyte containing the biosensor, followed by addition of incrementally increasing aliquots (2, 4, 10 and 50 μL) of fibrinogen and the response from the biosensor for each incremental plasminogen and fibrinogen addition was recorded.

Human serum albumin (HSA) obtained as a lyophilized powder was dissolved in PBS containing 5mM each of potassium ferrocyanide and potassium ferricyanide to obtain a stock concentration of 3.5% (normal serum albumin level in blood and plasma). In separate experiments, incrementally increasing aliquots (0.6, 6, 60 and 600 μL) of this stock solution of HSA, were first incrementally added to 6mL of the electrolyte containing the biosensor, followed by incremental addition of fibrinogen aliquots (2, 4, 10 and 50 μL) and the response from the biosensor for each incremental HSA and fibrinogen addition was recorded.

Residual fibrinogen content in the as-received samples of plasminogen, HSA, defibrinated human serum and human whole blood, was first determined using a human fibrinogen ELISA kit. Then, 0.2 mL serum or the whole blood was added to 9 mL of the electrolyte containing the biosensor, followed by incremental addition of fibrinogen aliquots (2, 4, 10, 50 and 100 μL) and the response from the biosensor for each incremental fibrinogen addition in this serum or whole blood containing electrolyte was recorded.

All data was saved in ASCII text format and exported to Microsoft Excel 2007 for Nyquist plot preparation and analysis of charge transfer characteristics. The data was also exported to ZView (Scribner Associates, Southern Pines, NC, USA) for equivalent circuit modeling. These simulations utilized a modified Randle's equivalent circuit, to extract important impedimetric parameters, and in particular, the changes in charge transfer resistance (ΔR_{ct}), in a manner consistent with previous reports (Singal *et al*. 2015, Wang *et al*. 2011). Please refer to supplementary information, Fig. S6 for the equivalent circuit utilized to model biosensor response. Supplementary information, Fig. S7 and Table S2, provides an example equivalent circuit simulation for the response of our fibrinogen biosensor to fibrinogen in whole blood.

3. Results and Discussion

3.1. Characterization of 12HC antibody attached graphene *via* FT-IR spectroscopy

Infrared spectra of the aminated and antibody-conjugated graphene sheets are depicted in Fig. 3. The aminated graphene exhibits the usual FTIR peaks, sharp at 1575 $cm^{-1}$and broad at 3350 cm^{-1}, consistent with the presence of primary amines. Upon the addition of 12HC antibodies, however, amide peaks appeared at 1650 cm^{-1} and 1560 cm^{-1} with broad NH and OH bands at 3440 cm^{-1} and 3180 cm^{-1}, respectively. The FTIR spectra confirm the presence of the 12HC antibodies bound to the graphene material. Additional corroborative evidence for the covalent nature of the attachment of 12HC antibodies to the graphene surface is provided in the supplementary information, Fig. S2.

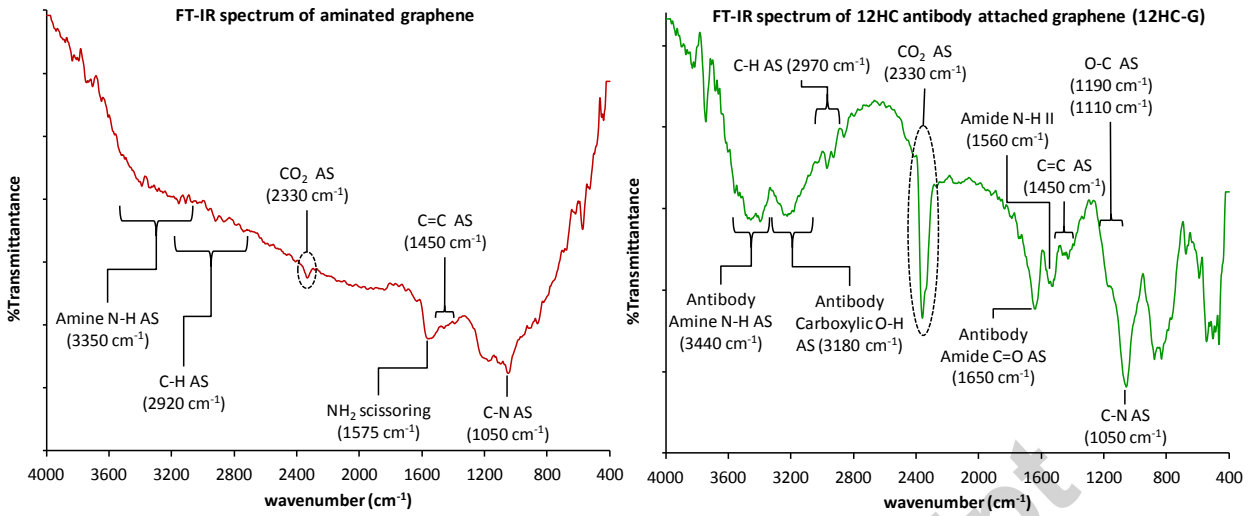

Fig. 3 FT-IR spectra of starting aminated graphene (left) and the final 12HC-G (right) materials which strongly suggest that 12HC antibodies are present on the graphene scaffold in the 12HC-G material.

3.2 Response of the fibrinogen biosensor to fibrinogen in simple aqueous matrix

The fibrinogen biosensor comprised of the 12HC-G material deposited on the screen printed electrodes can be utilized to sense fibrinogen from simple aqueous matrices using EIS spectroscopy. Fig. 4 (A and B) with overlaid Nyquist plots depicts a representative experiment whereby the 12HC-G biosensor was challenged with 863 to 4315 μg/dL of fibrinogen. As the fibrinogen concentration in the electrolyte increases, more antibody sites will be occupied with fibrinogen. This process progressively hinders the charge transfer process for the reversible one-electron outer sphere ferrocyanide/ferricyanide redox reaction that is occurring at the electrode. ZView simulations enabled extraction of the actual R_{ct} value at each fibrinogen challenge concentration. A plot of average ΔR_{ct} *vs.* $\log_{10}$ fibrinogen concentration (shown in Fig. 4C) for three separate biosensors and three separate bare graphene electrodes (N=3) reveals that while the 12HC-G biosensors responded to incrementally increasing fibrinogen challenge by displaying monotonically increasing charge transfer resistance, the bare graphene electrodes showed negligible response.

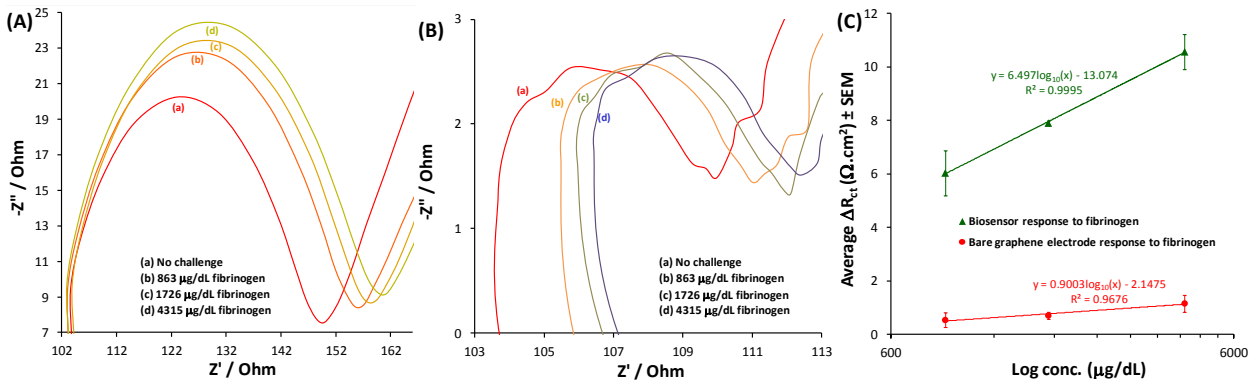

Fig. 4. (A) Representative overlaid Nyquist plots showing response of the fibrinogen biosensor to increasing fibrinogen challenge in simple aqueous medium. (B) Representative overlaid Nyquist plots of bare (no antibody) graphene electrode, showing that the antibody is essential for response to fibrinogen challenge. (C) Overlaid average ΔR_{ct} vs. $\log_{10}$ fibrinogen concentration plots showing that the fibrinogen biosensor specifically responds to increasing fibrinogen challenge, but the bare graphene electrode does not. (N = 3)

3.3. Fibrinogen sensing in the presence of plasminogen, a related coagulation cascade biomolecule and in the presence of high background serum albumin protein content with the fibrinogen biosensor

The fibrinogen biosensor appears to be selective for fibrinogen. Physiological concentrations of plasminogen, a related biomolecule involved in the coagulation cascade, do not appear to interfere with the response of the biosensor to fibrinogen. Fig. 5 depicts a representative experiment, during which the biosensor was first challenged with incrementally increasing concentrations of plasminogen until its concentration reached normal physiologic levels. This was followed by addition of known amounts of fibrinogen into the electrolyte. The change in the charge transfer resistance of the biosensor was essentially negligible (~ 0.5 $\Omega.cm^2$), in the presence of physiologically relevant concentration (4315 µg/dL) of plasminogen *i.e.* the biosensor is highly selective to fibrinogen over plasminogen. It is unlikely that this negligible background signal is from residual fibrinogen content in the plasminogen since ELISA based

interrogation of the as-obtained plasminogen revealed essentially negligible fibrinogen content (~0.26 μg/dL). Note however, that the biosensor responded, as expected, to fibrinogen by monotonically increasing the charge transfer resistance as a function of the fibrinogen challenge levels, in the presence of physiological concentrations of plasminogen.

Furthermore, as also depicted in Fig. 5, it was demonstrated that the biosensor could specifically sense fibrinogen in the presence of human serum albumin (HSA) background. The biosensor was first challenged with incrementally increasing amounts of HSA until the HSA concentration reached 0.35 g/dL, which is about 10% of the normal human blood plasma serum albumin levels, simulating the response to a minimally processed human sample. This was followed by addition of known amounts of fibrinogen into the electrolyte. Note that HSA produced a negligible non-specific ΔR_{ct} signal (~ 0.5 $\Omega.cm^2$). However, such small background signals from such electrochemical sensors in such high background protein levels are a very common observation. For example, very similar background responses of other graphene based immunosensors (Singal *et al*. 2015) and aptasensors (Wang *et al*. 2011) that utilize EIS based signal readout approaches comparable to our own, have been previously reported. It is unlikely that this background signal is from residual fibrinogen content in the HSA since ELISA based interrogation of the as-obtained HSA revealed essentially negligible fibrinogen content (~0.43 μg/dL).

These results strongly suggest that our biosensor may be suitable for sensing and quantifying fibrinogen from complex matrices (*e.g.* serum, plasma and blood) which also contain large amounts of related and unrelated proteins and other biomolecules.

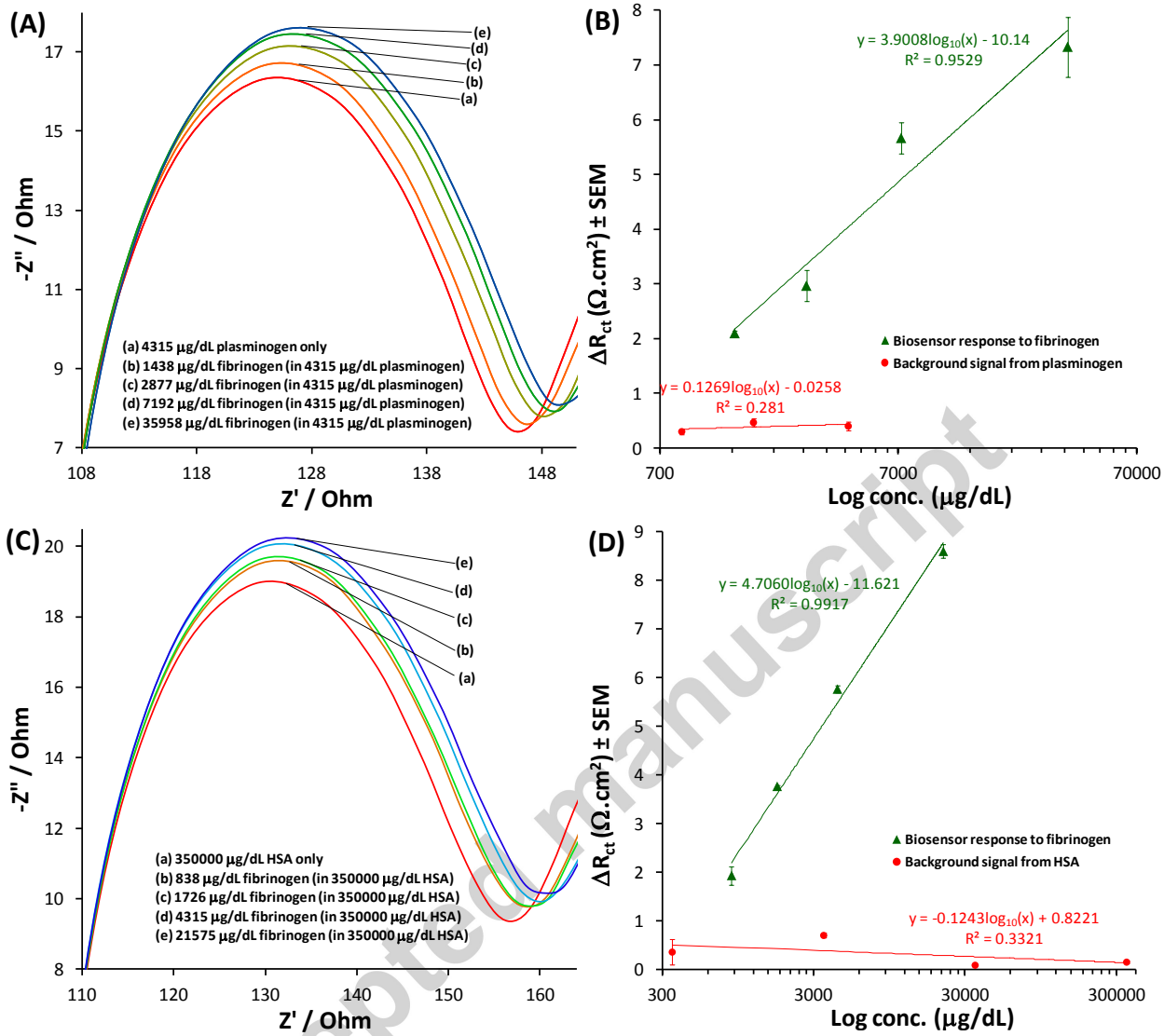

Fig. 5. (A) Representative overlaid Nyquist plots showing response of the fibrinogen biosensor to increasing plasminogen challenge followed by increasing fibrinogen challenge. (B) Average ΔR_{ct} vs. $\log_{10}$ concentration plots (N=3) showing that the fibrinogen biosensor specifically responds to increasing fibrinogen challenge, even in the presence of plasminogen. (C) Representative overlaid Nyquist plots showing response of the fibrinogen biosensor to increasing HSA challenge followed by increasing fibrinogen challenge. (D) Average ΔR_{ct} vs. $\log_{10}$ concentration plots (N = 2) showing that the fibrinogen biosensor specifically responds to increasing fibrinogen challenge, even in the presence of high background HSA content.

3.4. Fibrinogen sensing in human serum and unprocessed human whole blood samples with the fibrinogen biosensor

The fibrinogen biosensor reliably responds to fibrinogen in both human serum as well as in unprocessed human whole blood as depicted in Fig. 6. Quantification using a standard ELISA kit indicated that the residual fibrinogen content in the human serum (~ 2 μg/dL) and in the human blood samples (~ 3 μg/dL) obtained from the vendor (Innovative Research) were essentially negligible. For biosensor evaluations in these samples, 0.2 mL of these human serum and (in separate experiments) blood samples were added to 9 mL of the electrolyte comprised of PBS with 5 mM each of potassium ferrocyanide and potassium ferricyanide in the miniature electrochemical cell housing the biosensor. This was followed by incremental addition of fibrinogen to these serum or blood containing electrolyte solutions and subsequent recording of the EIS spectra after each addition. Note that the response of the biosensor to fibrinogen, under these conditions of challenge, is similar to the biosensor response to fibrinogen in high background HSA content. This is expected, because both serum and blood have significant amounts of serum albumins as well as other biomolecular content. Importantly, the observation that the biosensor has the potential to sense and quantify fibrinogen in human serum and unprocessed human whole blood is extremely encouraging. Consequently, the potential implications of our biosensor for continuous point-of-care fibrinogen monitoring are obvious. Specifically, we envision a multi-spot biosensor array in a fluidic cartridge for clinical fibrinogen monitoring in trauma patients. A whole blood sample collected from the patient can be introduced into the cartridge and be utilized to challenge a biosensor spot and the response will be recorded. The next blood sample from the same patient will challenge a fresh biosensor spot in the same cartridge and so on. The output will be a running fibrinogen trend which could

enable the clinician to more accurately control fibrinogen replacement therapy and positively influence patient outcomes by reversing trauma induced coagulopathy or preventing its onset.

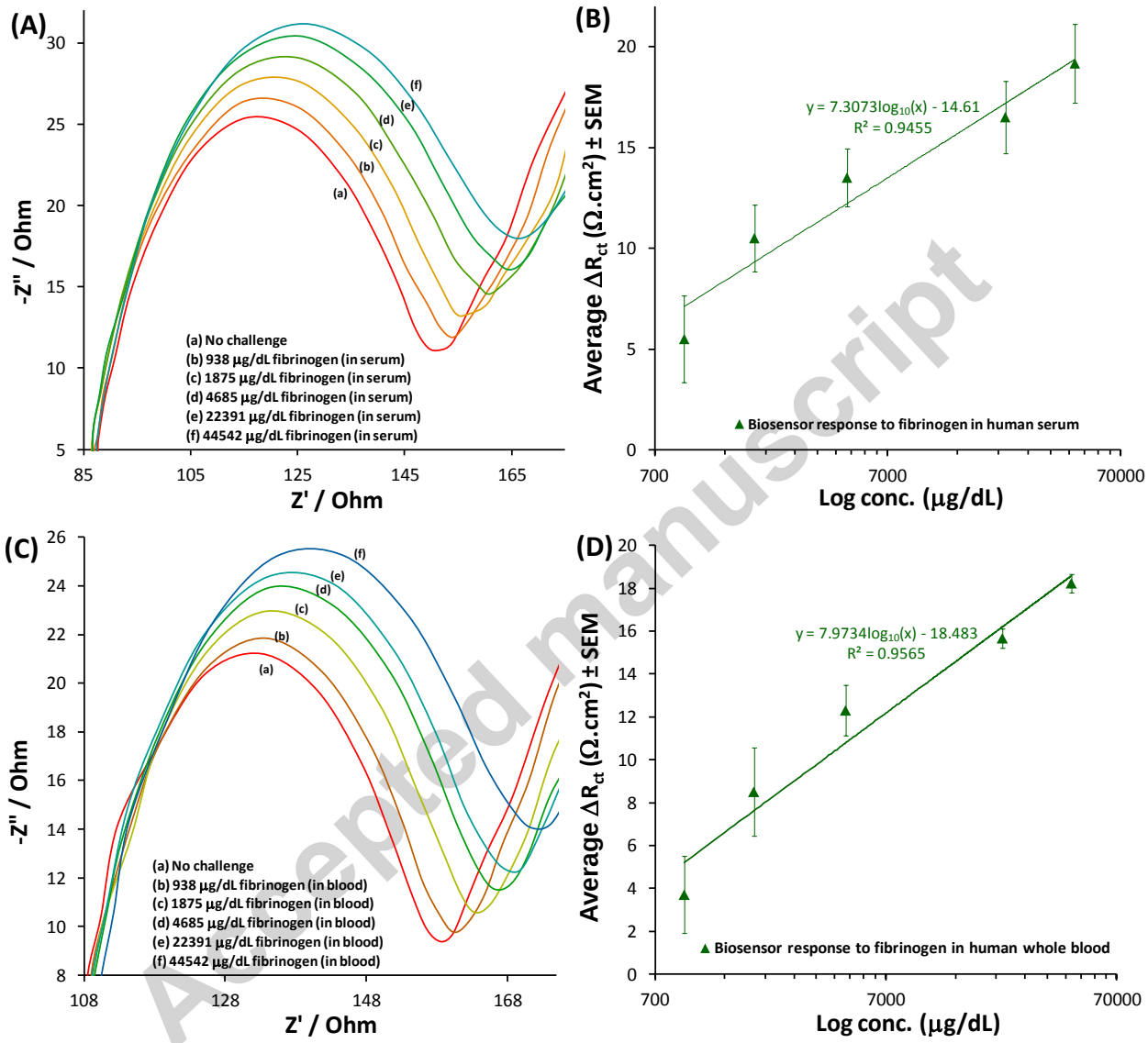

Fig. 6. (A) Representative overlaid Nyquist plots showing response of the fibrinogen biosensor to fibrinogen from human serum. (B) Average ΔR_{ct} vs. $\log_{10}$ concentration plots (N = 3) showing that the fibrinogen biosensor can sense fibrinogen from human serum. (C) Representative overlaid Nyquist plots showing response of the fibrinogen biosensor to fibrinogen from human whole blood. (D) Average ΔR_{ct} vs. $\log_{10}$ concentration plots (N = 3) showing that the fibrinogen biosensor can sense fibrinogen from human blood.

4. Conclusions

We have developed an antibody immobilized graphene-based electrochemical sensor for label-free immunosensing of fibrinogen, an important indicator of trauma induced coagulopathy. This biosensor has been prepared using simple chemistry and relatively inexpensive materials and methods. This biosensor has been shown to reliably and reproducibly sense levels of fibrinogen over the entire clinically relevant range of concentrations encountered in healthy subjects as well as in coagulopathic patients. The biosensor has been demonstrated to be selective for fibrinogen and appears capable of functioning well in the presence of potentially interfering species and high background protein content. Finally, the demonstration that this biosensor can sense fibrinogen from human serum and human whole blood samples is very important. These results will serve as the rationale to design similar impedimetric graphene based biosensors for other important indicators of trauma-induced coagulopathy *e.g.* antithrombin. We eventually envision multiplexing these biosensors for simultaneous real-time monitoring of these indicators so that caregivers can be empowered with actionable information which can enable them to better manage the treatment of traumatically injured patients. This in turn, is expected to enable them to greatly reduce the risk of, or completely prevent morbidity and mortality associated with coagulopathy in trauma patients.

Although this study provides preliminary *in vitro* support for the potential of our fibrinogen biosensor for clinical fibrinogen monitoring, it should be noted that the fibrinogen biosensors reported herein are still largely unoptimized. This is reflected in the fairly large variances in their responses to fibrinogen spiked in serum and whole blood samples. Therefore, at the present time, the ΔR_{ct} *vs.* log Fibrinogen plots have significantly hindered utility as

calibration curves for the determination of fibrinogen concentrations from unknown samples. Note however, that even unoptimized, these biosensors do appear to have the potential to grossly profile the trend in fibrinogen concentrations from actual blood samples. This functionality has potential clinical relevance in identifying the onset of coagulopathy to guide therapeutic intervention, as well as monitoring patient response following fibrinogen replacement therapy. Biosensor optimization to reduce variance in their responses, large replicate set evaluation and biosensor stability and shelf life evaluations will be the major focus of our research going forward.

Acknowledgements

This work is supported by the US Army Medical Research and Materiel Command under Contract No.W81XWH-15-C-0152. The views, opinions and/or findings contained in this report are those of the authors and should not be construed as an official Department of the Army position, policy or decision unless so designated by other documentation. We are grateful to Jeffrey Parkey and Dr. Xuguang Li for invaluable advice on biosensor fabrication and EIS spectroscopy for measuring biosensor response. We are also grateful to Dr. Mahesh Waje for helpful discussions on equivalent circuit modeling and EIS spectra fitting to extract impedimetric parameters. We gratefully acknowledge pertinent information freely provided by Prof. John Holcomb and Prof. Charles Wade on the clinical implications of continuous monitoring of indicators of trauma induced-coagulopathy and the limitations of the current clinical methods of fibrinogen quantification. We thank Dr. Wilbur Malloy for providing specific information on the implications of continuous monitoring of indicators of trauma induced-coagulopathy for tactical combat casualty care.

References

Brohi, K., Cohen, M. J., Ganter, M. T., Schultz, M. J., Levi, M., Mackersie, R. C., Pittet, J. F. 2008. J. Trauma 64(5), 1211-1217.

D'Angelo, M. R., Dutton, R. P. 2010. AANA J. 78(1), 35-40.

Fries, D., Martini, W. Z. 2010. Br. J. Anesthesia 105(2), 116-121.

Liu, Y., Dong, X., Chen, P. 2012. Chem. Soc. Rev. 41, 2283-2307.

Loo, A. H., Bonanni, A., Pumera, M. 2012. Nanoscale, 4, 143-147.

Meyer, M. A. S., Ostrowski, S. R., Sorensen, A. M., Meyer, A. S. P., Holcomb, J. B., Wade, C. E., Johansson, P. I., Stensballe, J. 2015. J. Surg. Res., 194(2), 581-590.

Nardi, G., Agostini, V, Maria, B. R., Bocci, G., Di Bartolomeo, S., Bini, G., Chiara, O., Cingolani, E., De Blasio, E., Gordini, G., Coniglio, C., Pellegrin, C., Targa, L., Volpi, A. 2013. Anesthesiology Clin. Sci. doi: 10.7243/2049-9752-2-22.

Parkey, J., Cross, J., Hayes, R., Parham, C., Staack, D., Sharma, A. C. 2015. Plasma Processes Polym. 12, 1244-1255.

Pusateri, A. E. 2012. US Department of Defense Hemorrhage and Resuscitation Research and Development Program, in Remote Damage Control Resuscitation (RDCR) Conference, Bergen, Norway.

Sauaia, A.; Moore, F. A., Moore, E. E., 1995. J. Trauma 38(2), 185-193.

Sharma, A. C., Jana, T., Kesavamoorthy, R., Shi, L., Virji, M. A., Finegold, D. N., Asher, S. A. 2004. J. Am. Chem. Soc. 126(9), 2971-2977.

Singal, S., Srivastava, A. K., Dhakate, S., Biradar, A. M., Rajesh 2015. RSC Adv. 5, 74994-75003.

Stinger, H. K., Spinella, P. C., Perkins, J. G., Grathwohl, K. W., Salinas, J., Martini, W. Z., Hess, J. R., Dubick, M. A., Beekley, A. C., Wolf, S. E., Wade, C. E., Holcomb, J. B. 2008. J. Trauma 64(2), S79-S85.

Undas, A. 2016. Seminars in Thrombosis and Hemostasis 42(2), 381-388.

Wan, Y., Lin, Z., Zhang, D., Wang, Y., Hou, B. 2011. Biosens. Bioelectron. 26, 1959-1964.

Wang, Z., Zhang, J., Chen, P., Zhou, X., Yang, Y., Wu, S., Niu, L., Han, Y., Wang, L., Chen, P., Boey, F., Zhang, Q., Liedberg, B., Zhang, H. 2011. Biosens. Bioelectron. 26, 3881-3886.

HIGHLIGHTS

- An antibody immobilized graphene based biosensor for fibrinogen has been developed.
- The biosensor reliably and reproducibly senses fibrinogen from aqueous media.
- Biosensor selectivity for fibrinogen is maintained in the presence of potential interferents such as other coagulation cascade molecules and high serum albumin protein background.
- The biosensor can effectively sense fibrinogen over the entire clinically relevant range (938 – 44542 μg/dL) in human serum and unprocessed human whole blood.

HIGHLIGHTS

- An antibody immobilized graphene based biosensor for fibrinogen has been developed.
- The biosensor reliably and reproducibly senses fibrinogen from aqueous media.

- Biosensor selectivity for fibrinogen is maintained in the presence of potential interferents such as other coagulation cascade molecules and high serum albumin protein background.

- The biosensor can effectively sense fibrinogen over the entire clinically relevant range (938 – 44542 μg/dL) in human serum and unprocessed human whole blood.